This document is the accepted manuscript version of the following article:
Gröning, O., Stolz, S., Prinz, J., Brune, H., & Widmer, R. (2022). When a molecular motor does the quantum leap. Europhysics News, 53(4), 24-27.
https://doi.org/10.1051/epn/2022405

When a molecular motor does the quantum leap

Oliver Gröning[a], Samuel Stolz[a,b], Jan Prinz[a,b], Harrald Brune[b], Roland Widmer[a]

[a] Empa, Swiss Federal Laboratories for Materials Science and Technology, 8600 Dübendorf (Switzerland)

[b] Institute of Physics, École Polytechnique Fédérale de Lausanne, 1015 Lausanne (Switzerland)

In his seminal 1959 lecture "There's Plenty of Room at the Bottom" Richard Feynman has put forward two challenges.[1] The first was to shrink letters to a size, which allowed writing the whole Encyclopedia Britannica on the head of a pin - which was achieved in 1985.[2] The second challenge read: "It is my intention to offer a prize of $1,000 to the first guy who makes a rotating electric motor which can be controlled from the outside and, not counting the lead-in wires, is only 1/64th inch cubed."[1] Less than a year later, William McLellan met this challenge by scaling down an electric motor consisting of just 13 parts and weighing some 250 μg to the required size.[3]

Motivated by the ubiquity of nanoscale machines in biology, the desire to achieve ever smaller sizes remained vivid and the first motors brought to molecular dimensions were reported in 1999.[4,5] To this day, most synthetic molecular machines, although driven by quantum processes such as light absorption and bond reconfiguration,[6] exhibit classical kinetics. This contrasts with quantum mechanical real space tunneling. As illustrated in Fig. 1, instead of a quasi-continuous classical trajectory, the process of a particle overcoming a potential barrier by tunneling looks more like an abrupt leap. In a quantum system, having determined a particle's position at time t_0 by measurement, its wave function will subsequently spread out over time, such that it acquires a non-zero probability to be in places, where it would be classically forbidden. When the position of the particle is measured at a later time t_1 and its wave function collapses with non-zero probability in the adjacent well, it might thus seem to have "tunneled" through the potential barrier.

For quantum mechanical tunneling to occur with non-vanishing rates the requirements are that the energy barrier between the initial and final configuration is small, the tunneling distance short, the mass of the system in motion light, and the operation temperature low. To give an idea of the scales: on a copper surface a hydrogen atom with mass m_H = 1.67e-27 kg tunnels a distance of 2.55 Å (= 2.55e-10 m) across a potential barrier of about 0.2 eV (= 3.2e-20 J) with an average rate of about once every 40 minutes[9]. Scaling down a unidirectional molecular motor to meet the requirements for real space tunneling is therefore a formidable challenge.

Like an ordinary electric motor, our atomic motor consists of a stator and a rotor. As we want to achieve a directional motion, either the stator or the rotor should show a handedness or chirality, which makes a clockwise (CW) rotation inequivalent to a counter-clockwise (CCW) turn. An atomic cluster of the surface of a chiral Palladium-Gallium (PdGa) crystal realizes our chiral stator[7,8]. Figure 2a shows its pinwheel-like atomic structure, which consists of 3 central Palladium atoms (light blue), which are surrounded by deeper layers of 6 Gallium (red) and 3 Palladium atoms (dark blue). Having a chiral stator allows us to use very small and symmetric rotors such as a single rod-shaped acetylene (C_2H_2) molecule with a length of about 3.3 Å and a mass of 26 Dalton (= 4.32e-26 kg). The motor self-assembles by exposing the PdGa surface to acetylene gas (at 10e-9 mbar) at low temperatures (below 170 K). Figure 2b shows the scanning tunneling microscopy (STM) image of such a motor at 77 K. The three-lobed bright feature in the center shows a rotating acetylene molecule, where the rotation is much faster than the frame rate of the STM (about one frame per minute). This means the image represents a time average of the molecule in all its meta-stable rotation states as schematically shown on the right hand side of Fig. 2b).

Only by reducing the temperature to 5 K, the rotation becomes slow enough for the STM to image the molecule in each of its 3 distinguishable rotational states (see. Fig. 3a and 3b). One can see that from one frame to the other that the acetylene molecule rotates by 60° in the CCW direction with a bit of eccentricity.

As the frame rate of STM is rather slow, we use a different mode of observation, which drastically increases the time resolution. As shown schematically in Fig. 3c, instead of constantly imaging the acetylene molecule, we 'park' the tip of the STM at a certain position over the molecule. In the 'parking' mode, each rotation of the molecule changes the current between the tip and the sample. Figure 3d shows such a current-time diagram with the tip parked in the position denoted by the marker in right-most image of Fig. 3a. This time series is characterized by 3 distinct current levels (A, B and C), each corresponding to one rotational state of the rotor, and sudden transitions, i.e. jumps, between them. Based on the distance between the molecule and the tip, we can correlate the current levels with the rotational states observed in the STM topographies (see Fig. 3a). What is remarkable is that the sequence of rotational transitions from A to B to C and back to A, which corresponds to a 180° rotation, is maintained throughout the whole sequence of the 23 rotation-events, which implies unidirectional CCW motion of the rotor. Under the best conditions, the probability of a jump in the wrong direction is about 1%.

As mentioned before, the rotation rate or rotation frequency is temperature dependent and Fig. 4a shows this dependency in more detail. From about 15 K onwards, we see that there is an exponential increase of the rotation frequency, from which we can deduce an energy barrier height between the rotation states of about 25 meV. We estimate that at 77 K (see Fig. 2b) the rotor spins faster than 100'000 times a second. All temperature induced rotations are, however, not directional. This is in accordance with the 2nd law of thermodynamics. As we control temperature macroscopically, the stator, the rotor and the STM tip are in thermal equilibrium and a thermally activated, directional motion is impossible because it would decrease entropy.

The rotation of the rotor, however, is not just activated by temperature; the tunneling current of the STM can induce rotation events too. Figure 4b shows the rotation rate as a function of the bias voltage between tip and sample at a constant current of 100 pA. As for the temperature dependence, we observe a sharp increase of the rotation frequency above a threshold of about 35 mV independent of polarity. In contrast to

the non-directed rotation induced by temperature, the rotations induced by the STM current are directional for voltages slightly above the threshold. With increasing voltage, the direction of the rotations become progressively random. The fact that there is linear relationship between the STM current and the rotation frequency implies that a single electron transfers some of its energy to the rotor, which enables it to overcome the potential barrier between two rotation states. This is a very rare event and only about 1 out 1 billion electrons flowing through the motor actually triggers a rotation. Directionality is enabled due to friction as the rotor requires a little bit less activation energy to overcome the barrier in the CCW direction. The reason is that the trajectory in the CW direction is a bit shorter (a result of the stator being chiral) and the rotor loses less energy on this path as compared to the CW one, thus resulting in a directional rotation at low activation energies.

So far, we have been discussing the classical motion of the motor and we can understand it in terms of Arrhenius' law when it is temperature activated or Newton's mechanics with friction when it is electrically stimulated. However, if we turn our attention back to Figures 4a and 4b, we see that below the threshold temperature and voltage (i.e. in the non-shaded regions of the diagrams), the rotation frequency does not decrease, but remains constant. This is the signature of the quantum-tunneling regime, which is at first glance astonishing because the acetylene rotor is massive, 26 times heavier than the hydrogen atom tunneling on a copper surface. However, for the rotation it is not the mass, which is relevant but the moment of inertia, which is about 5.6e-46 kgm^2. Furthermore, with 25 meV the potential barrier is small and we expect a higher tunneling rate than for H on copper. Lastly, there is also an experimental test if this can be quantum tunneling. By replacing the hydrogen atoms in the acetylene by deuterium, we increase the moment of inertia by only 20%, but the tunneling rate however, drops by a factor of 4. This extreme sensitivity agrees with the theoretical expectations for quantum tunneling.[7,9]

Open questions, however, remain. The rotation in the tunneling regime is directional too, which is surprising, because an asymmetrically skewed rotation potential alone

does not yield asymmetric tunneling rates. From fundamental thermodynamic considerations, the directional tunneling motion must be related to dissipative processes. Further investigation, e.g. by ultra-fast STM, are needed to elucidate the relationships between atomic friction and directional tunneling.

Acknowledgements

The original article of this work was published in June 2020 in the Proceedings of the National Academy of Sciences of the United States of America 117(26), 14838 (2020) (https://doi.org/10.1073/pnas.1918654117) and funding from the Swiss National Science Foundation under SNSF Project grants 20002-159690 and 200021-129511 is gratefully acknowledged.

Figure Captions:

Figure 1

Illustrative comparison of a classical (left) and a quantum tunneling (right) transition from one minimum of a potential energy landscape to another.

Figure 2

a) Schematic representation of the atomic structure of the stator (blue balls represent Pd and red ones Ga atoms) and the rotor of the motor. b) STM image of a fast-rotating C_2H_2 molecule at 77 K, with the schematic representation of the time-averaged configuration of the rotor as inset.

Figure 3

a) STM images and b) the corresponding atomistic models of one acetylene molecule on the Pd_3:A surface in its three distinct, energetically equivalent, 60° rotated states. c)

Schematic illustration of the experimental setup to probe and drive the acetylene on Pd_3:A molecular motor with an exemplary experimental current-time sequence in d). A time-lapse movie of the rotation can be found here: https://www.youtube.com/watch?v=g7COlp6hK3A.

Figure 4

The dependence of our molecular motor's rotation frequency and directionality on a) temperature and b) applied bias voltage. The red and grey shaded regions in a) and b) denote the thermally and electrically activated rotation respectively; in the non-shaded regions, the non-zero constant rotation frequency shows tunneling characteristics.

References

1. Feynman, R. P., Leighton, R. B. & Sands, M. The Feynman Lectures on Physics. vol. 1 (Addison-Wesley, 1963).
2. Newman, T. H., Williams, K. E. & Pease, R. F. W. High resolution patterning system with a single bore objective lens. J. Vac. Sci. Technol. B Microelectron. Process. Phenom. 5, 88–91 (1987).
3. Feynman, R. Infinitesimal machinery. J. Microelectromechanical Syst. 2, 4–14 (1993).
4. Nagatoshi Koumura, R. W. J. Z., Richard A. van Delden, N. H. & Ben L. Feringa. Light-driven monodirectional molecular motor. Nature 401, 152–155 (1999).
5. Kelly, T. R., De Silva, H. & Silva, R. A. Unidirectional rotary motion in a molecular system. Nature 401, 150–152 (1999).
6. Salma Kassern, T. van L., Anouk S. Lubbe, M. R. W. & Ben L. Feringa, D. A. L. Artificial molecular motors. Chem Soc Rev 46, 2592–2621 (2017).
7. Stolz, S., Gröning, O., Prinz, J., Brune, H. & Widmer, R. Molecular motor crossing the frontier of classical to quantum tunneling motion. Proc. Natl. Acad. Sci. 117, 14838–14842 (2020).
8. Prinz, J. et al. Isolated Pd sites on the intermetallic PdGa(111) and PdGa(-1-1-1) model catalyst surfaces. Angew. Chem. 124, 9473–9477 (2012).
9. Lauhon, L.J. & Ho, W. Direct Observation of the Quantum Tunneling of Single Hydrogen Atoms with a Scanning Tunneling Microscope. Phys. Rev. Lett. 85, 4566-4569 (2000)

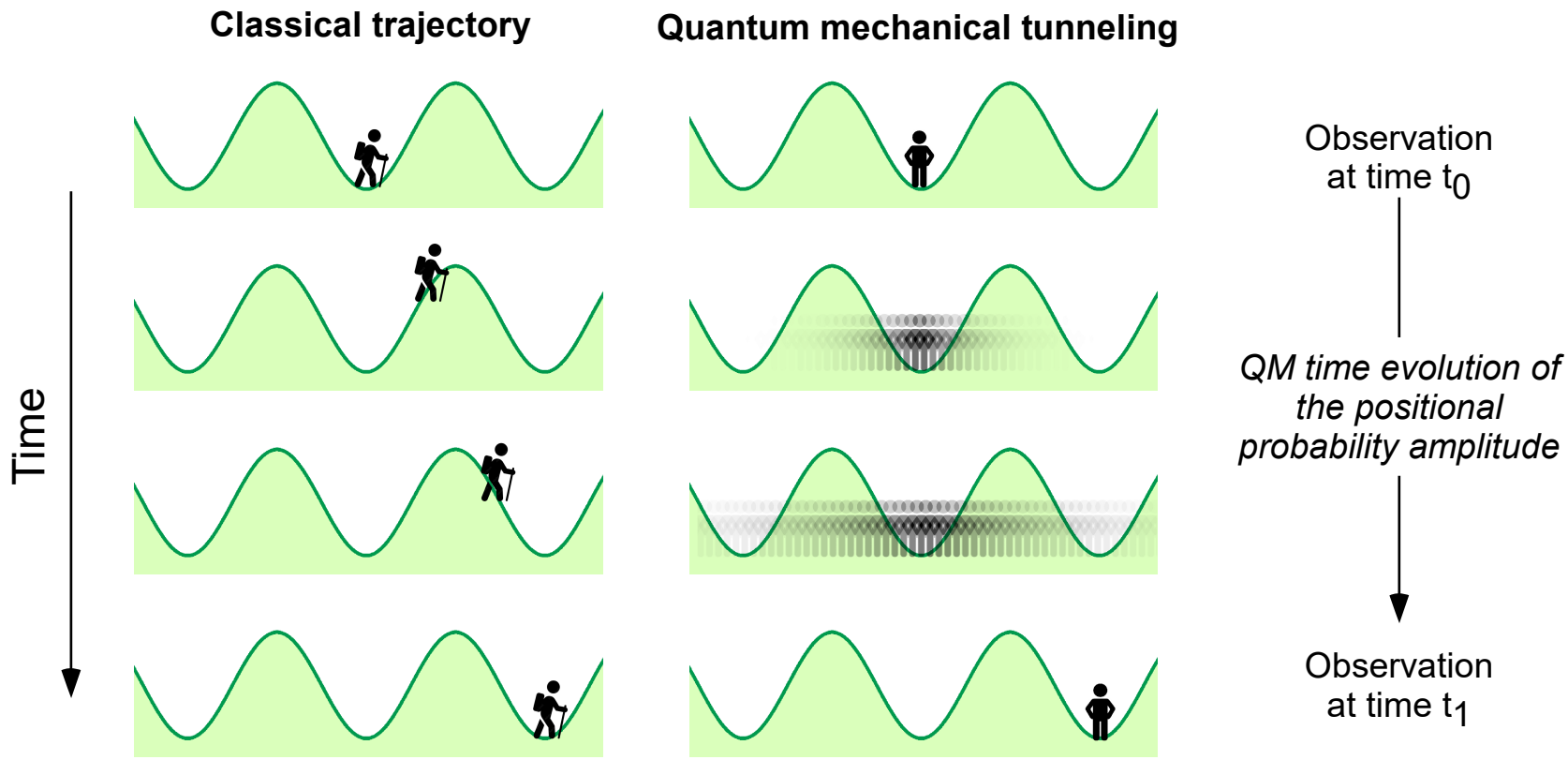
Classical trajectory
Quantum mechanical tunneling
Time
Observation at time t_0
QM time evolution of the positional probability amplitude
Observation at time t_1

Figure 1

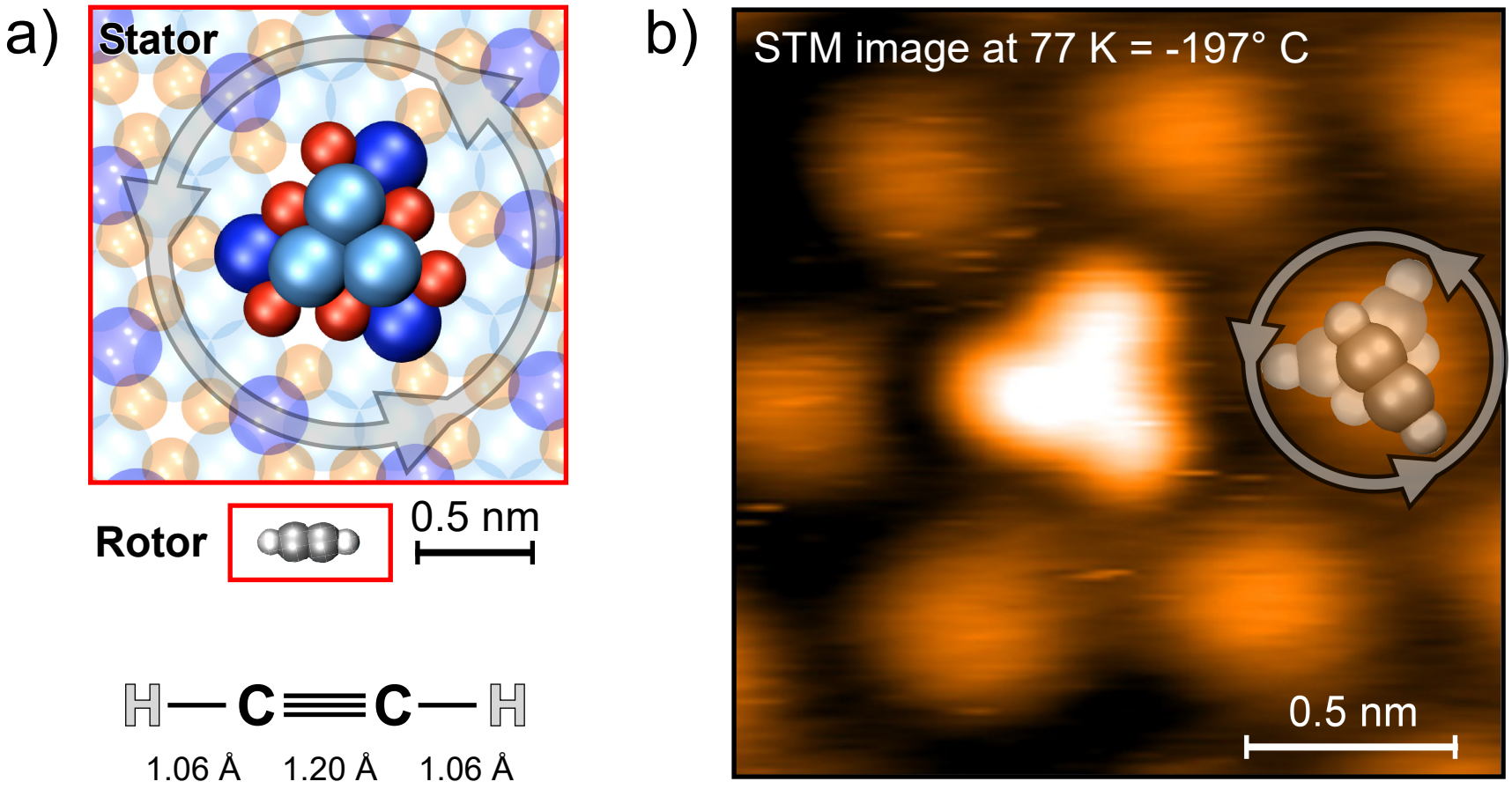
a)
Stator
Rotor
0.5 nm
H—C≡C—H
1.06 Å
1.20 Å
1.06 Å
b)
STM image at 77 K = -197° C
0.5 nm

Figure 2

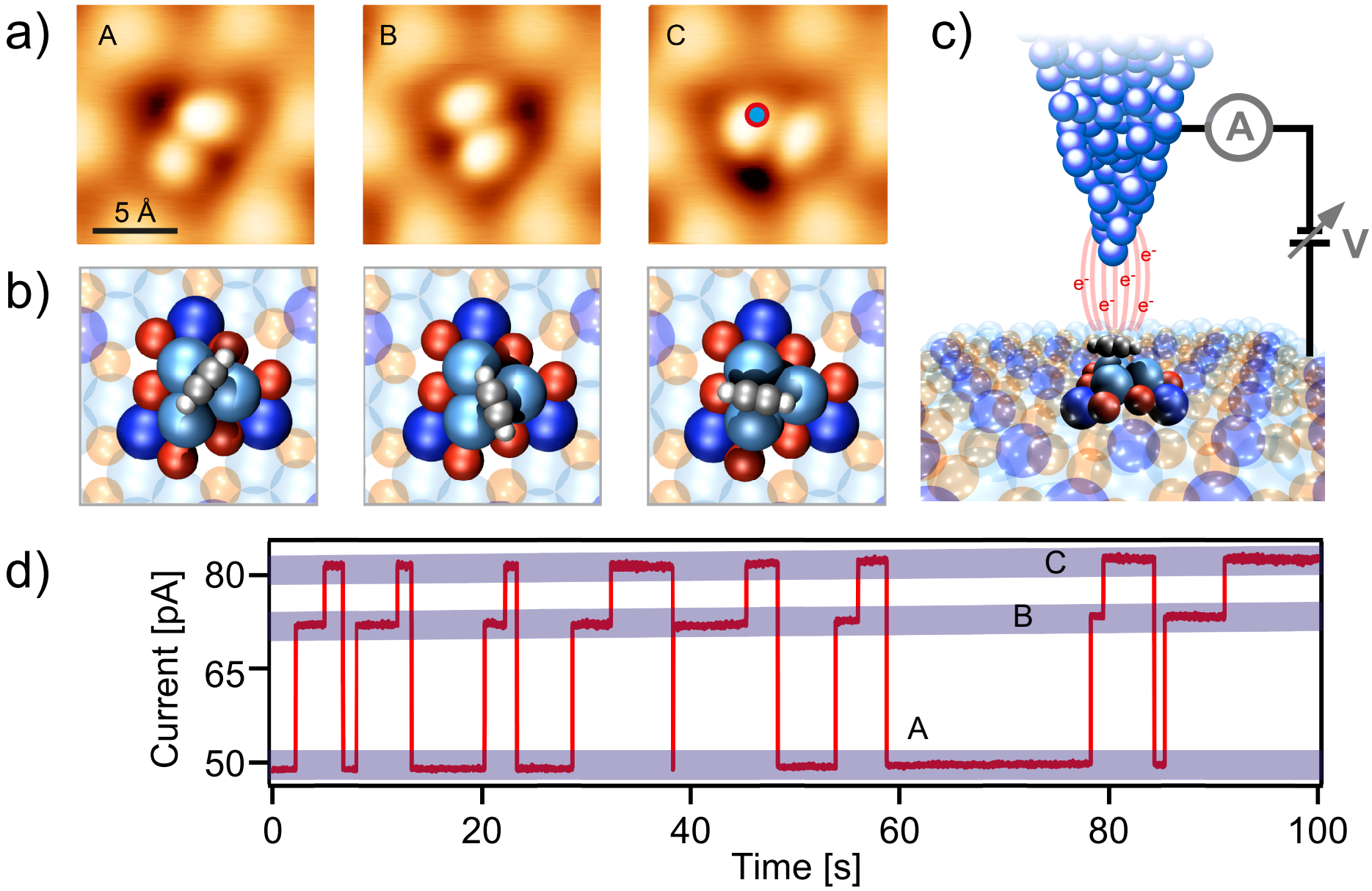
a)
A
B
C
5 Å
b)
c)
A
V
e-
e-
e-
e-
e-
d)
Current [pA]
80
65
50
C
B
A
0
20
40
60
80
100
Time [s]

Figure 3

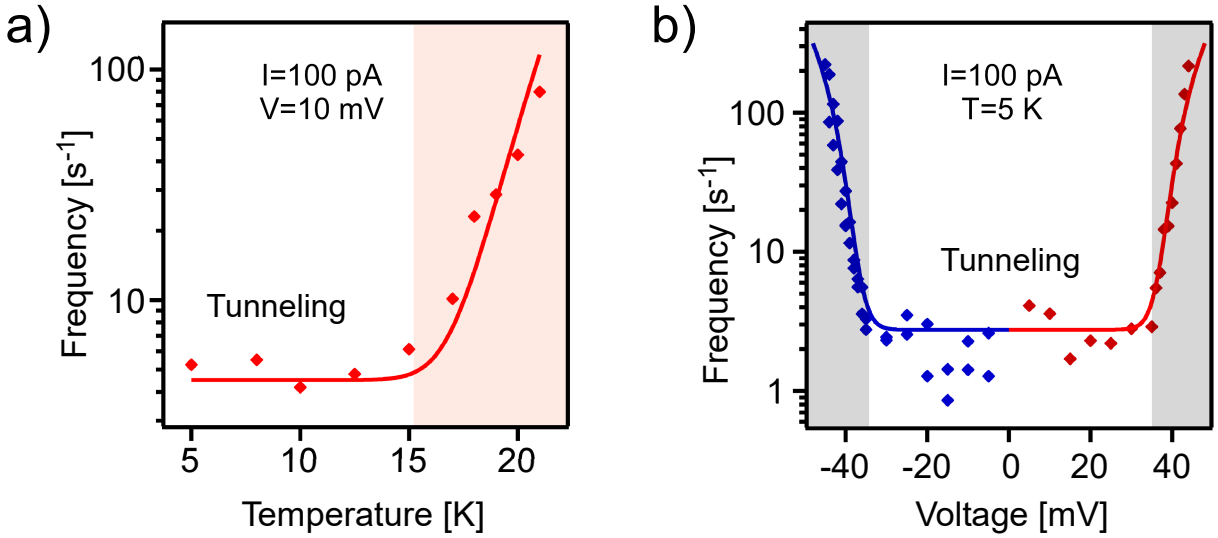
a)
I=100 pA
V=10 mV
Tunneling
Frequency [s-1]
100
10
5
10
15
20
Temperature [K]
b)
I=100 pA
T=5 K
Tunneling
Frequency [s-1]
100
10
1
-40
-20
0
20
40
Voltage [mV]

Figure 4